Investigación *Revista Mexicana de Física* **33** *No. 4(1988) 599–630*

Generalized additional boundary conditions for nonlocal thin films

J.A. Gaspar-Armenta

Centro de Investigación en Física de la Universidad de Sonora, Apdo. postal A–088, 83190 Hermosillo, Son.

P. Halevi

Departamento de Física del Instituto de Ciencias, Universidad Autónoma de Puebla, Apdo. postal J–48, 72570 Puebla, Pue.

(recibido el 12 de febrero de 1987; aceptado el 4 de junio de 1987)

Abstract. We calculate the generalized additional boundary conditions (ABC's) for a non-local dielectric film interacting with s-polarized light. These ABC's correspond to a recently introduced parameter U that describes, macroscopically, the interaction between an excitation and the surfaces of the non-local medium. With group II–VI semiconductors in mind, we also allow for exciton-free layers at the two surfaces of the thin film. The reflectivity, transmittivity, and absorptivity for CdS are calculated by means of an approach that utilizes a sequence of surface impedances. These spectra exhibit a series of resonances which are consequences of an interference between four plane waves in the non-local medium. Some of the resonances may be interpreted in terms of Fabry–Perot standing waves. The strongest non-local effects are obtained for $U = -1$ (the Pekar ABC), and the weakest for $U = 1$ (the Fuchs–Kliewer or Ting–Frankel–Birman ABC). We also find that spectra of thin films are strongly affected by the presence of dead layers. A comparison with an experimental spectrum by Makarenko, Uraltsev and Kiselev favors the value $U \simeq -0.5$.

Resumen. Calculamos las condiciones a la frontera generalizadas (ABC's) para una película dieléctrica no-local que interactúa con luz de polarización s. Estas ABC's corresponden a un parámetro U recientemente introducido que describe, macroscópicamente, la interacción entre una excitación y las superficies del medio no-local. Estando nuestro interés dirigido hacia semiconductores del grupo II–VI también incluimos capas libres de excitones ("muertas") en las dos superficies de la película delgada. La reflectividad, transmitividad y absortividad para CdS son calculados mediante un enfoque que utiliza una secuencia de impedancias de superficie. Estos espectros exhiben una serie de resonancias que son consecuencias de interferencia entre cuatro ondas planas en el medio no-local. Algunas de las resonancias pueden ser interpretadas en términos de resonancias Fabry–Perot de ondas estacionarias. Los efectos no-locales más fuertes se obtienen para $U = -1$ (el ABC de Pekar) y los más débiles para $U = 1$ (el ABC de Fuchs–Kliewer o de Ting–Frankel–Birman). También encontramos que los espectros de las películas delgadas son fuertemente afectados por la presencia de capas muertas. Una comparación con un espectro experimental de Makarenko, Uraltsev y Kiselev favorece el valor $U \simeq -0.5$.

PACS: 78.65.Jd; 78.40.Ha; 73.60.Fw

1. Introduction

This paper is concerned with the generalized additional boundary condition (ABC) for non-local dielectrics, mainly semiconductors of the II–VI group that possess a direct excitonic transition. A former paper by Halevi and Fuchs [1], (denominated I) introduced the basic model and gave a calculation of the reflectivity for a simple surface. A second paper by the same authors [2] dealt with surface polaritons. In the present paper we will apply the model introduced in I to non-local thin films interacting with s-polarized light.

The principal advantage in utilizing thin films, rather than massive crystals, is the possibility of amplifying the non-local effects by means of Fabry–Perot resonances. It will be remembered that, for s-polarized light, two plane waves may simultaneously propagate in the spatially dispersive (non-local) medium. For the same value of the frequency ω one of these waves has a much greater wavevector $\mathrm{Re}\, q$ than the other wave. It is possible to choose the thickness of the film in such a way that this "non-local wave" will have an increased importance. The actual positions of the peaks in the spectrum depends, in a complicated way, on the dispersion relation $\omega(q)$, the thickness of the film, the ABC, and the thicknesses of the exciton-free ("dead") layers.

Kiselev *et al.* [3] measured the reflection and transmission spectra of several films of CdS and CdSe in the regions for the A- and B-excitons. By fitting theoretical curves based on the ABC of Pekar [4] to the experimental ones these authors were able to determine the parameters in the dielectric function $\epsilon(\omega)$ (Eq. (I.1)). In the vicinity of the longitudinal exciton frequency ω_L the fit was improved by allowance for a dead layer, originally postulated by Hopfield and Thomas [5]. Bishop [6] calculated reflection and transmission spectra for three different ABC's and found qualitative differences; she has also considered the effect of exciton-free layers. In a calculation involving *p*-polarized light incident on a thin film of CdS Johnson [7] called attention to a structure in the reflectivity spectrum that disappears for normal incidence; this effect is caused by a longitudinal wave. Makarenko *et al.* [8] took various reflectivity spectra of thin films of CdS in the region of the A-exciton and obtained the corresponding material parameters by fitting with the Pekar ABC. The fit is quite good, however the authors assumed that the phenomenological damping frequency ν has a value up to five times greater for $\omega > \omega_L$ than for $\omega < \omega_L$. The aforementioned authors find that the discontinuity in ν is greater for smaller thicknesses, which is attributed to an energy-loss canal associated with the surfaces.

In this paper we utilize the generalized ABC in order to obtain the reflectivity R, the transmittivity T, and the absorptivity A. Included in the calculation are dead layers at both surfaces. Reliable values of the parameters for the $A(n = 1)$ exciton of CdS have been determined by means of resonant Brillouin scattering (RBS) by Yu and Evangelisti [9]. This leaves us with the following adjustable parameters: the damping frequency ν, the thickness l of the exciton-free layer, and the parameter U that characterizes the generalized ABC.

In section 2 we describe the dielectric response of a non-local thin film and show that the excitonic polarization $P(z)$ obeys the ABC of I (for s-polarization) at both interfaces between the spatially dispersive bulk and the two exciton-free layers. In section 3 we calculate the surface impedance of the five-layer structure (vacuum-dead layer-non-local bulk-dead layer-vacuum) and we obtain the corresponding expressions for R and T. In section 4 R, T and A are displayed graphycally as function of the frequency ω, the angle of incidence θ, and the thickness d of our CdS film. In this section we also included a comparison between theoretical spectra for several values of the parameter U and an experimental spectrum by Makarenko *et al.* [8]. This parameter U is given the values -1 corresponding to the Pekar ABC; 0 corresponding to the Agarwal *et al.* [10] ABC; 1 corresponding to the Fuchs-Kliewer [11] or Ting *et al.* [12] ABC; and the non-integral values ± 0.5. Our results are discussed in section 5.

2. Dielectric response of a spatially dispersive thin film

In this section we confine our attention to the non-local bulk region $l < z < d-l$; the dead layers on both sides will be included in the following section. We only consider s-polarized light, therefore longitudinal modes are not excited. Thus we have to deal with the two transverse modes. The reader is referred to I for details of the notation and the basic formulas.

The dielectric response of the non-local region is given by the following model susceptibility function:

$$\chi(z, z') = \chi_B(z - z') + \chi_S(z, z'). \tag{1}$$

Here $\chi_B(z - z')$ is the Fourier transform (I.17) of the bulk susceptibility $\chi(q_z)$; it depends only on the distance between the points z and z' and is thus insensitive to surface effects. Therefore $\chi_B(z-z')$ gives the non-local bulk response. The second term in Eq. (1) is defined as

$$\chi_S(z, z') = \sum_{n=1}^{\infty} U^n\{\chi_B(\varsigma_n) + \chi_B(\varsigma_n')\}, \tag{2}$$

where now the arguments ς_n and ς_n' of the function χ_B are the projections on the z-axis of the trajectories followed by the exciton (or, possibly, another excitation) after n interactions with the surface. Here ς (ς') refers to the case that the first interaction, as we proceed from the point of excitation $\mathbf{r}'$ to the point of observation $\mathbf{r}$, takes place at the surface $z = l$ ($z = d - l$). The first few values of ς_n and ς_n' are illustrated in Fig. 1. As in I, the phenomenological parameter U describes the strength of the interaction between the excitation and the surfaces. If U is raised to the n'th power it means that n interactions have taken place. Equations (1) and (2) constitute a generalization of Eq. (I.16) to the thin film geometry. The quantities ς_n and ς_n' describe the phase changes, in the direction perpendicular to the film, of the exciton for a given scattering process "n". According to Eq. (I.22),

$$\chi_B(\varsigma_n) = \frac{\epsilon_0 - 1}{4\pi}\,\delta(\varsigma_n) + \frac{i\omega_p^2}{8\pi D\Gamma}\,e^{i\Gamma|\varsigma_n|} \tag{3}$$

with $\Gamma(\omega)$ given by Eq. (I.10),

$$\Gamma = \{(\omega^2 - \omega_T^2 - Dq_x^2 + i\nu\omega)/D\}^{1/2}. \tag{4}$$

Here q_x is the component of the wavevector parallel to the surface, ω_T is the transverse frequency of the exciton, $D = h\omega_T/(m_e + m_h)$, ϵ_0 is the background dielectric constant, ω_p is a measure of the oscillator strength, and ν is the phenomenological damping frequency.

The wavevectors of the two transverse modes are given by Eq. (I.19). In an unbounded medium this equation has two solutions for the normal component q_z, namely q_1 and q_2. In our bounded medium, however, we must also include the reflected waves with the solutions $-q_1$ and $-q_2$. For this reason the electric field in the spatially dispersive region is expected to have the form

$$\begin{aligned} E(\mathbf{r},t) = \Big\{ & E^{(+1)}e^{iq_1 z} + E^{(+2)}e^{iq_2 z} + E^{(-1)}e^{-iq_1 z} \\ & + E^{(-2)}e^{-iq_2 z}\Big\} e^{i(q_x x - \omega t)}, \qquad (l \le z \le d - l). \end{aligned} \tag{5}$$

Because we are considering s-polarized light, and the plane of incidence is the XZ plane, Eq. (5) actually gives the (only) y-component of the field. Using the notation of Eq. (I.14) we write $E(\mathbf{r},t) = E(z)\exp[i(q_x x - \omega t)]$, etc. Thus

$$E(z) = \sum_{k=1}^{2} \left\{ E^{(+k)} e^{iq_k z} + E^{(-k)} e^{-iq_k z} \right\}. \tag{5a}$$

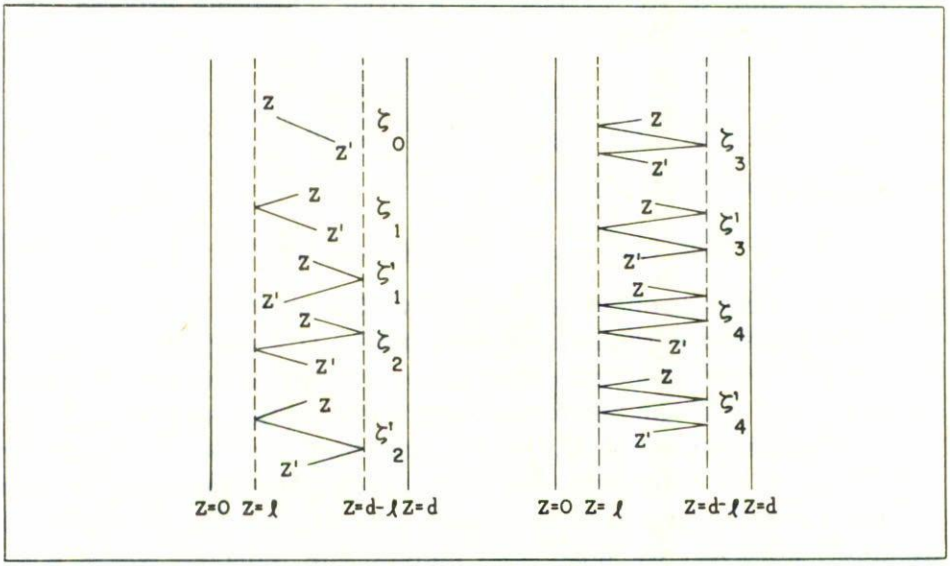

FIGURE 1. An exciton in "created" at the point $\mathbf{r}'$ and "observed" at the point $\mathbf{r}$ in the non-local medium. It may proceed from $\mathbf{r}'$ to $\mathbf{r}$ directly, giving rise to a bulk process, or else it may interact with one or both surface layers any number of times. The possible processes are schematically indicated. The normal components of $\mathbf{r}$ and $\mathbf{r}'$ are z and z', and they are measured from the left-hand surface. The quantities ς_n and ς_n' are the projections on the z-axis of the trajectories followed by the excitation after n interactions with the surface; for each value of n there are two possible processes.

By Eqs. (1) and (5a) the polarization in the spatially dispersive medium is

$$P(z) = \int_l^{d-l} \chi(z,z')E(z')\,dz' = \sum_{k=1}^{2} \int_l^{d-l} \Big\{ \chi_B(z-z') + \chi_S(z,z') \Big\} \times \Big\{ E^{(+k)} e^{iq_k z'} + E^{(-k)} e^{-iq_k z'} \Big\}\, dz'. \tag{6}$$

According to Eqs. (2) and (3) the functions $\chi_B(z-z')$ and $\chi_S(z,z')$ are

$$\chi_B(z-z') = \frac{\epsilon_0 - 1}{4\pi}\,\delta(z-z') + \frac{i\omega_p^2}{8\pi D\Gamma}\, e^{i\Gamma|z-z'|} \tag{7}$$

and

$$\chi_S(z,z') = \frac{i\omega_p^2}{8\pi D\Gamma} \sum_{n=1}^{\infty} U^n \Big(e^{i\Gamma\varsigma_n} + e^{i\Gamma\varsigma_n'} \Big). \tag{8}$$

As ς_n and ς_n' are positive quantities the Dirac delta function does not appear in the last equation. After substituting in Eq. (8) the ς_n and ς_n' as given in Fig. 1 the summation may be performed, to yield the result

$$\chi_S(z,z') = \frac{i\omega_p^2 U\, e^{i\Gamma(d-2l)}}{8\pi D\Gamma[1 - U^2 e^{2i\Gamma(d-2l)}]} \Big\{ [e^{i\Gamma(z+z'-d)} + e^{-i\Gamma(z+z'-d)}] + U e^{i\Gamma(d-2l)} [e^{i\Gamma(z-z')} + e^{-i\Gamma(z-z')}] \Big\}. \tag{9}$$

Next we substitute Eqs. (7) and (9) in Eq. (6) and perform the integration, giving

$$P(z) = \frac{\epsilon_0 - 1}{4\pi} E(z) + \frac{\omega_p^2}{8\pi D\Gamma} \sum_{k=1}^{2} \left\{ \left(\frac{1}{q_k - \Gamma} - \frac{1}{q_k + \Gamma} \right) \times \left[E^{(+k)} e^{iq_k z} + E^{(-k)} e^{-iq_k z} \right] - \left[\frac{M_k e^{i\Gamma(z-l)} + N_k e^{-i\Gamma(z+l-d)}}{1 - U^2 e^{2i\Gamma(d-2l)}} \right] \right\}, \tag{10}$$

where

$$M_k = \left[a(q_k) + a(-q_k) U e^{i(\Gamma+q_k)(d-2l)} \right] E^{(+k)} e^{iq_k l} + \left[a(-q_k) + a(q_k) U e^{i(\Gamma-q_k)(d-2l)} \right] E^{(-k)} e^{-iq_k l} \tag{11}$$

and

$$N_k = \left[a(-q_k) + a(q_k) U e^{i(\Gamma-q_k)(d-2l)} \right] E^{(+k)} e^{iq_k (d-l)} + \left[a(q_k) + a(-q_k) U e^{i(\Gamma+q_k)(d-2l)} \right] E^{(-k)} e^{-iq_k (d-l)} \tag{12}$$

$$a(q_k) = \frac{1}{q_k - \Gamma} + \frac{U}{q_k + \Gamma}. \tag{13}$$

If we substitute Eqs. (5a) and (10) in the wave equation (I.13) then we find terms that are proportional to $\exp(iq_1 z)$, $\exp(-iq_1 z)$, $\exp(iq_2 z)$, $\exp(-iq_2 z)$, $\exp(i\Gamma z)$, and $\exp(-i\Gamma z)$. The wave equation must be satisfied for an arbitrary value of z (between l and $d - l$) and therefore the coefficients of all these terms must vanish. We see from Eq. (10) that the coefficients of $\exp(i\Gamma z)$ and $\exp(-i\Gamma z)$ are proportional, respectively, to $\sum M_k$ and $\sum N_k$. Thus we conclude that

$$\sum_{k=1}^{2} M_k = \sum_{k=1}^{2} N_k = 0. \tag{14}$$

Substituting from Eqs. (11) and (12) we get

$$\sum_{k=1}^{2}\left[a(q_k)E^{(+k)}e^{iq_k l}+a(-q_k)E^{(-k)}e^{iq_k l}\right]$$
$$+\,Ue^{i\Gamma(d-2l)}\sum_{k=1}^{2}\left[a(-q_k)E^{(+k)}e^{iq_k(d-l)}+a(q_k)E^{(-k)}e^{-iq_k(d-l)}\right]=0$$

and

$$\sum_{k=1}^{2}\left[a(-q_k)E^{(+k)}e^{iq_k(d-l)}+a(q_k)E^{(-k)}e^{-iq_k(d-l)}\right]$$
$$+\,Ue^{i\Gamma(d-2l)}\sum_{k=1}^{2}\left[a(q_k)E^{(+k)}e^{iq_k l}+a(-q_k)E^{(-k)}e^{-iq_k l}\right]=0$$

Because $U^2\exp[2i\Gamma(d-2l)]\neq 1$ the last two equations may be satisfied only if each of the two sums vanishes

$$\sum_{k=1}^{2}\left[a(q_k)E^{(+k)}e^{iq_k l}+a(-q_k)E^{(-k)}e^{-iq_k l}\right]=0 \tag{15}$$

and

$$\sum_{k=1}^{2}\left[a(-q_k)E^{(+k)}e^{iq_k(d-l)}+a(q_k)E^{(-k)}e^{-iq_k(d-l)}\right]=0. \tag{16}$$

These are the desired generalized ABC's. They are relations that must be obeyed by the electric field at the planes $z=l$ and $z=d-l$, respectively.

The generalized ABC's may also be expressed in terms of the excitonic polarization $\mathcal{P}(z)$ that excludes the polarization of the background dielectric. By using Eqs. (10) and (14) we find that

$$\begin{aligned}\mathcal{P}(z)&=P(z)-[(\epsilon_0-1)/4\pi]E(z)\\&=\frac{\omega_p^2}{4\pi D}\sum_{k=1}^{2}\left\{\frac{1}{q_k^2-\Gamma^2}\left[E^{(+k)}e^{iq_k z}+E^{(-k)}e^{-iq_k z}\right]\right\}.\end{aligned} \tag{17}$$

By substituting Eq. (13) in Eq. (15) we get

$$\begin{aligned}(1+U)\sum_{k=1}^{2}\frac{q_k}{q_k^2-\Gamma^2}\left[E^{(+k)}e^{iq_kl}-E^{(-k)}e^{-iq_kl}\right]\\+(1-U)\Gamma\sum_{k=1}^{2}\frac{1}{q_k^2-\Gamma^2}\left[E^{(+k)}e^{iq_kl}+E^{(-k)}e^{-iq_kl}\right]=0.\end{aligned}\tag{18}$$

It is easy to show that the first sum is equal to $(4\pi D/i\omega_p^2)\{\partial \mathcal{P}/\partial z\}_{z=l}$ and that the second sum is equal to $(4\pi D/\omega_p^2)\mathcal{P}_{z=l}$. Hence Eq. (18) reduces to

$$i\Gamma(1-U)\mathcal{P}(l)+(1+U)\,d\mathcal{P}(l)/dz=0.\tag{19}$$

In the same way Eq. (16) leads to

$$i\Gamma(1-U)\mathcal{P}(d-l)-(1+U)\,d\mathcal{P}(d-l)/dz=0.\tag{20}$$

Equations (19) and (20) are the generalized ABC for the excitonic polarization at the interfaces $z=l$ and $z=d-l$. Note that these equations are essentially the same as Eq. (I.31). The only differences are that, in the presence of the dead layers $\mathcal{P}(z)$ is evaluated at $z=l$ and $z=d-l$, rather than at $z=0$, and the obvious change in sign of the second term in Eq. (20).

It is interesting that the ABC's Eqs. (19) and (20) are independent of the width of the non-local region.

3. Optical properties of thin films

We have a system composed of five plane parallel layers: vacuum with a dielectric constant $\epsilon=1$ $(z<0)$, an exciton-free surface layer characterized by the background dielectric constant $\epsilon=\epsilon_0$ $(0<z<l)$; the bulk with the non-local dielectric constant $\epsilon=\epsilon(\omega,q)$ $(l<z<d-l)$; the exciton-free layer on the other side of the film

with $\epsilon = \epsilon_0$ $(d-l < z < d)$; and again vacuum having $\epsilon = 1$ $(z > d)$. The fields in these media must have the form

$$E(z) = E_I e^{iq_0 z \cos\theta} + E_R e^{-iq_0 z \cos\theta}, \qquad z \le 0; \tag{21a}$$

$$E(z) = E_1^{(+)} e^{iq_l z} + E_1^{(-)} e^{-iq_l z}, \qquad 0 \le z \le l; \tag{21b}$$

$$E(z) = \sum_{k=1}^{2} \left[E^{(+k)} e^{iq_k z} + E^{(-k)} e^{-iq_k z} \right], \qquad l \le z \le d-l; \tag{5a}$$

$$E(z) = E_2^{(+)} e^{iq_l z} + E_2^{(-)} e^{-iq_l z}, \qquad d-l \le z \le d; \tag{21c}$$

$$E(z) = E_T e^{iq_0 z \cos\theta}, \qquad z \ge d. \tag{21d}$$

Here $q_0 = \omega/c$ is the vacuum wavevector, $q_l = q_0(\epsilon_0 - \sin^2\theta)^{1/2}$ is the normal component of the wavevector in the dead layers, $q_k = q_1$ and $q_k = q_2$ are the two solutions of the equation $\epsilon(\omega, q) = q^2c^2/\omega^2$ and θ is the angle of incidence.

As is well known, the s-polarized reflectivity may be expressed in terms of a surface impedance Z as follows:

$$R = \left| \frac{Z - Z^{(0)}}{Z + Z^{(0)}} \right|^2, \tag{22}$$

where $Z^{(0)} = 1/\cos\theta$ is the surface impedance of vacuum, and

$$Z = -E_y(0^+)/B_x(0^+) \tag{23}$$

and the magnetic field is given by Faraday's law:

$$B_x = \frac{i}{q_0} \frac{dE_y(z)}{dz}. \tag{24}$$

Because $E_y(z)$ and $B_x(z)$ are both continuous quantities, so is their ratio and we may define a continuously varying surface impedance $Z(z)$. Then in Eq. (23), $Z = Z(0^+)$. Using Eqs. (23) and (24) and dropping the subscript y we write

$$Z(z) = iq_0 E(z)[dE(z)/dz]^{-1}. \tag{25}$$

The calculation may be performed by means of a scheme that involves a sequence of impedances. We express $Z = Z(0^+)$ in terms of $Z(l^+)$, then express $Z(l^+)$ in terms of $Z(d-l^+)$, and finally express $Z(d-l^+)$ in terms of $Z(d^+)$ which is, of course the surface impedance of vacuum. The calculation is based on the continuity of the field-components $E_y(z)$ and $B_x(z)$ at the interfaces $z = 0$, l, $d-l$, and d. The expressions for these fields are found from Eqs. (5a), (21a)–(21d), and (25). A considerable amount of algebra leads to the following sequence, derived in appendix A:

$$Z = Z(0^+) = \frac{q_0}{q_l}\,\frac{Z(l) - i(q_0/q_l)\tan q_l l}{(q_0/q_l) - iZ(l)\tan q_l l}, \tag{26}$$

$$Z(l) = q_0 \frac{b_1}{b_3}\,\frac{(b_1+b_2)Z(d-l) + q_0(b_1c_2/c_4 - b_2c_1/c_3)}{(b_3-b_4)Z(d-l) + q_0(b_3c_2/c_4 + b_4c_1/c_3)}, \tag{27}$$

$$Z(d-l) = \frac{q_0}{q_l}\,\frac{Z(d^+) - i(q_0/q_l)\tan q_l l}{(q_0/q_l) - iZ(d^+)\tan q_l l}, \tag{28}$$

$$Z(d^+) = Z^{(0)} = 1/\cos\theta. \tag{29}$$

The quantities b_i and c_i are given by Eq. (A.10).

The transmittivity is

$$T = |E_T/E_1|^2, \tag{30}$$

where it is shown in appendix B that

$$\begin{aligned} \frac{E_T}{E_1} = {} & \frac{2Ze^{-iq_0 d\cos\theta}}{Z + Z^{(0)}}\,\frac{Z(l)}{Z(l)\cos q_l l - i(q_0/q_l)\sin q_l l} \\ & \times \frac{Z(d-l)(c_1c_4 + c_2c_3)}{Z(d-l)(b_1c_4 + b_2c_3) + q_0(b_1c_2 - b_2c_1)} \\ & \times \frac{Z(d)}{Z(d)\cos q_l l - i(q_0/q_l)\sin q_l l}. \end{aligned} \tag{31}$$

Finally, the absorptivity is

$$A = 1 - R - T. \tag{32}$$

4. Numerical results

4.1. Comparison with other calculations

As a check on our calculations and computer program we made comparisons with theoretical results by Johnson [7] and Bishop [6]. We have calculated the normal incidence reflectivity for a 400 Å thick CdS film using the ABC's of Pekar and of Fuchs–Kliewer. Our results coincide with those of Johnson [7], except for small differences that are attributable to a slightly different set of parameters that we used.

On the other hand, our results for ZnSe are very different than those reported by Bishop [6] in spite of the fact that we have used the very same parameters quoted in her paper. We believe that the value of ω_p in her computer data was not the same as the value given in the paper.

4.2. Fabry–Perot resonances of the $A(n=1)$ exciton of CdS

In our calculations we have used the parameters for the $A(n=1)$ exciton of CdS determined by RBS by Yu and Evangelisti [9]. These are $\epsilon_0 = 9.1$. $m_e + m_h = 0.94 m_0$, $h\omega_T = 2,552.73$ meV, $\omega_L - \omega_T = 1.86$ meV, and $h\nu = 0.124$ meV. We have chosen the thicknesses of the dead layers as $l = 100$ Å each, and the overall thickness of the film as $d = 1,200$ Å. The parameter U is given the values 1, 0.5, 0, -0.5, and -1.

In local optics (and a transparent medium) it is well known [13] that minima are obtained in the reflection spectrum of a film of thickness L whenever the condition

$$q_L = n\pi, \qquad (n = 1, 2, 3, \ldots) \tag{33}$$

is fulfilled. Thus, for normal incidence, these "Fabry–Perot resonances" occur whenever an integer number of half-wavelenghts (π/q) fits into the thickness L. In case of oblique incidence q should be

n	ω_n (meV)	$\text{Re}\, q_k$	$\text{Im}\, q_k$	n	ω_n (meV)	$\text{Re}\, q_k$	$\text{Im}\, q_k$
1	2558.0	3.14	0.010	7	2554.6	22.00	0.340
2	2551.7	6.28	0.092	8	2555.2	25.13	0.302
3	2552.7	9.42	0.353	9	2555.9	28.27	0.270
4	2553.2	12.56	0.455	10	2556.6	31.42	0.245
5	2553.6	15.71	0.432	11	2557.5	34.56	0.222
6	2554.1	18.85	0.382	12	2558.4	37.70	0.204

TABLE I. The frequencies ω_n for which Eq. (34) is satisfied either for $k = 1$ (the "local wave") or for $k = 2$ (the "non-local wave"). $\text{Re}\, q_k$ and $\text{Im}\, q_k$ are given in $(10^3 \text{ Å})^{-1}$. The real and imaginary parts of the wavevector q_k are also given. Here we consider normal incidence and $d - 2l = 1,000$ Å. In the frequency region of interest only $n = 1$ corresponds to the "local wave", while all the other resonances, $2 \leq n \leq 12$ correspond to the "non-local wave".

replaced by the normal component q_z. Moreover, in our non-local medium there are two modes (labeled $k = 1, 2$) and this medium has a thickness $(d - 2l)$, so we expect that the above condition must be replaced by

$$\text{Re}\, q_k(d - 2l) = n\pi, \qquad k = 1, 2, \quad n = 1, 2, 3, \ldots \tag{34}$$

In table I we list the frequencies, within the range of interest, for which Eq. (34) is satisfied in the case of normal incidence. Similarly, table II gives the corresponding frequencies for s-polarized incidence with $\theta = 80°$. The columns for the imaginary part of q_k show that $\text{Im}\, q_k \ll \text{Re}\, q_k$, so absorption is not expected to be very important.

4.3. Reflection

The reflection spectra have been calculated from Eqs. (22) and (26)–(29). For normal incidence, $\theta = 0$, they are shown in Fig. 2. First we analyse the case $U = 1$ corresponding to the Fuchs–Kliewer or to the Ting *et al.* ABC. Outside the range (ω_T, ω_L) the spectrum

n	ω_n (meV)	$\mathrm{Re}\, q_k$	$\mathrm{Im}\, q_k$	n	ω_n (meV)	$\mathrm{Re}\, q_k$	$\mathrm{Im}\, q_k$
1	2560.1	3.14	0.005	7	2554.6	22.00	0.338
2	2551.8	6.28	0.105	8	2555.2	25.13	0.301
3	2552.7	9.42	0.365	9	2555.9	28.27	0.269
4	2553.2	12.56	0.456	10	2556.7	31.42	0.243
5	2553.6	15.71	0.432	11	2557.5	34.56	0.221
6	2554.1	18.85	0.383	12	2558.4	37.70	0.203

TABLE II. As in table I, however for s-polarized incidence with $\theta = 80°$

is very similar to that for the local case ($D = 0$) and the non-local behavior is confined to the region $\omega_T \leq \omega \leq \omega_L$. It was found by Gaspar–Armenta [14] that, in the absence of dead layers ($l = 0$), the five minima coincide in positions with the frequencies ω_2, ω_3, ω_4, ω_5 and ω_1 in table I. Here our allowance for finite dead layers causes substantial shifts from the predictions of the rather naive application of Eq. (34). Intuitively one may expect that the expression $(d-2l)$ in Eq. (34) should be replaced by some average of $(d-2l)$ and d, thus allowing for the fact that the thickness of the film is actually d. Then for a given n, Eq. (34) would be satisfied by a smaller value of $\mathrm{Re}\, q_k$, and as a result, smaller ω_n. Indeed, we observe in Fig. 2 a shift of the minima to lower frequencies: this effect is especially notable for $n = 1$, where $\Delta\omega \simeq -3$ meV. Incidentally, in the frequency range of interest, this resonance at $\omega \simeq \omega_L$ is the only one that is contributed by the "local wave".

As we decrease the parameter U, in steps of 0.5, from the value 1 in Fig. 2(b) to the value -1 in Fig. 2(f) three things happen. Firstly, the above discussed minima of Fig. 2(b) are gradually shifted to higher frequencies, secondly, some of the minima below ω_L disappear. Thirdly, oscillations of increasing amplitude appear above ω_L. In this region we expect that the minima are related to Fabry–Perot resonances of the "non-local wave" for high values of n. However, there is no obvious correspondence between the positions —and even

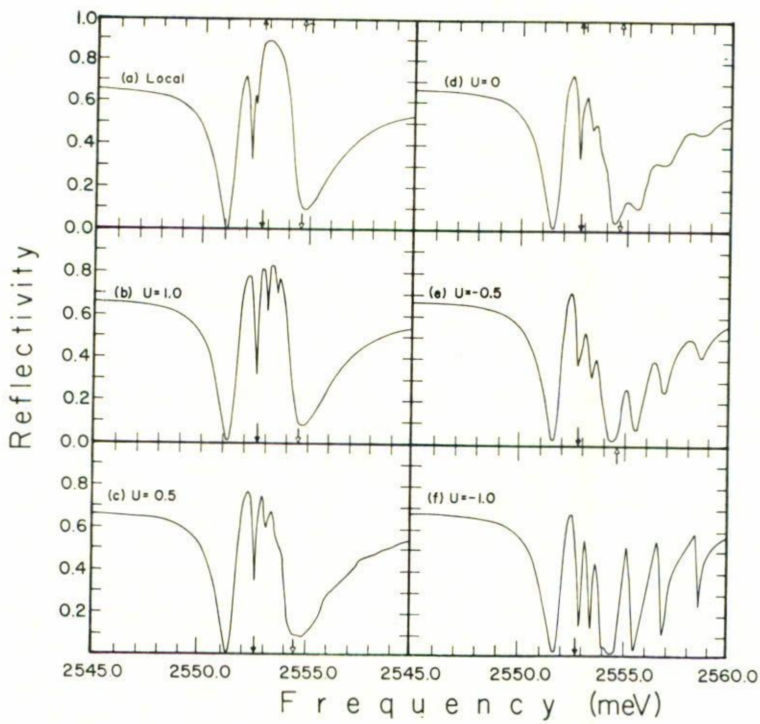

FIGURE 2. Normal-incidence reflectivity spectra $R(\omega)$ of CdS in the vicinity of the $A(n=1)$ exciton. The film thickness is 1,200 Å and exciton-free layers 100 Å thick have been included at both surfaces. Other parameters have been taken from Yu and Evangelisti [9]. The five values of U in (b)–(f) correspond to five ABC's. The local case $(D=0)$ is shown for comparison in (a).

number— of these minima and the ω_n in table I. This situation is unaltered even for $l=0$. Clearly, for $U \leq 0$ Eq. (34) is not very useful, because four, rather than two, plane waves (with wavevectors $\pm q_1$ and $\pm q_2$) participate in the process of interference. This is

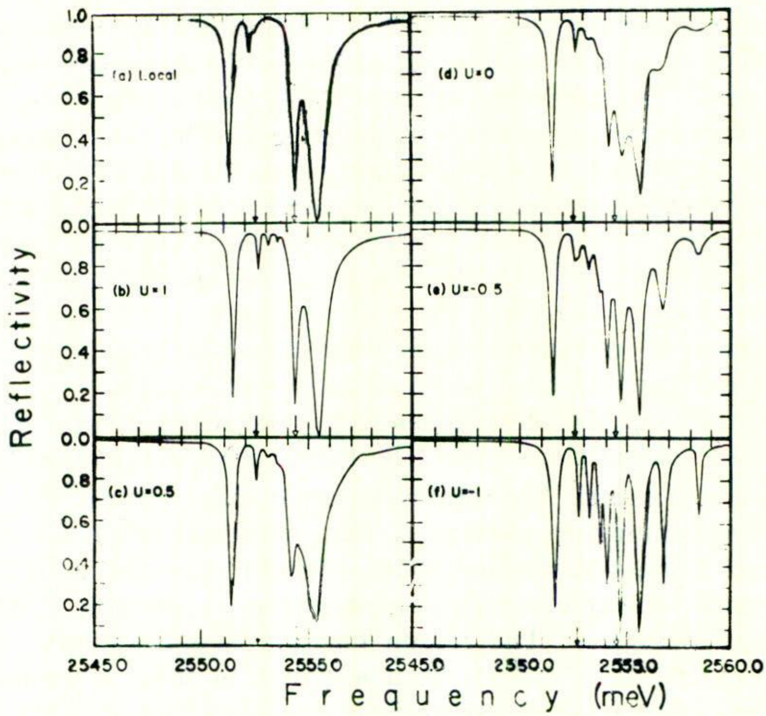

FIGURE 3. As in Fig. 2 for *s*-polarized light with an angle of incidence $\theta = 80°$.

to say that the non-local effects are very important; they are most dramatic for $U = -1$, that is, the Pekar ABC.

The case of *s*-polarized incidence, with $\theta = 80°$, is illustrated in Fig. 3. Many features of the normal-incidence spectrum, Fig. 2 are repeated. There are, however two notable differences. One is that now, generally speaking, the reflectivity values are greater (although the relative values of $R(\omega)$ for different minima are largely unaffected). This is to be expected: for an angle $\theta = 80°$ most of the incident light should be reflected provided that ω is not very near to a resonance frequency. The other difference is that the broad minimum in the vicinity of ω_L, for $\theta = 0$, splits into two minima, thus increasing by one the number of minima in the frequency range that we studied. The minimum at $\omega \simeq 2,556$ meV seems to be related to the Fabry–Perot resonance ω_1 in table II. The considerable shift must be explained by the participation of the "non-local wave" in the interference process, and by the presence of the dead layers. The minimum at $\omega \simeq \omega_L$ is associated with the "matching frequency" $\omega_M \simeq \omega_L$ introduced in I. This frequency is defined by the equation $\mathrm{Re}\,\epsilon(\omega = \omega_M, q = 0) = 1$. At $\omega = \omega_M$ for $\nu = 0$, $D = 0$ and in the absence of dead layers all the light should be transmitted. Thus, indeed, we may expect a minimum in the reflectivity.

Because Eq. (34) determines $\mathrm{Re}\,q_k$, the real part of the normal component of the wavevector, the third columns in tables I and II are clearly identical. The total wavevector is $(q_k^2 + q_0^2 \sin^2\theta)^{1/2}$; then the corresponding frequency ω_n may be found from the normal-incidence dispersion relation. Note, however, that the ω_n in table II are almost the same as the corresponding ω_n in table I, the only exception being ω_1. The reason for this is quite simple, namely $q_0 \sin\theta \simeq 1.3 \times 10^{-3}$ Å^{-1}; then a glance in table II reveals that $q_0 \sin\theta$ is quite small in comparison to all the $\mathrm{Re}\,q_k$ but $\mathrm{Re}\,q_1$. The dependence of $R(\omega)$ on the parameter U is similar in Figs. 2 and 3.

In Fig. 4 we show an example of an angular scan, fixing the frequency at $\omega = \omega_L$. In the local case, and for $U = 1$ and $U = 0$ a minimum exists at $\theta \simeq 55°$. However, for $U = -1$ the reflectivity is a monotously increasing function of θ. We find that the $R(\theta)$ curves strongly depend on the choice of ω and on the value of d.

We also exhibit the dependence of R on d (see Fig. 5) for normal incidence and $\omega = \omega_L$. The case $U = 1$ is very similar to the local case, while for $U = 0$ and $U = -1$ we obtain a complex structure that is related to the interference of the four waves with wavevectors $\pm q_1$ and $\pm q_2$.

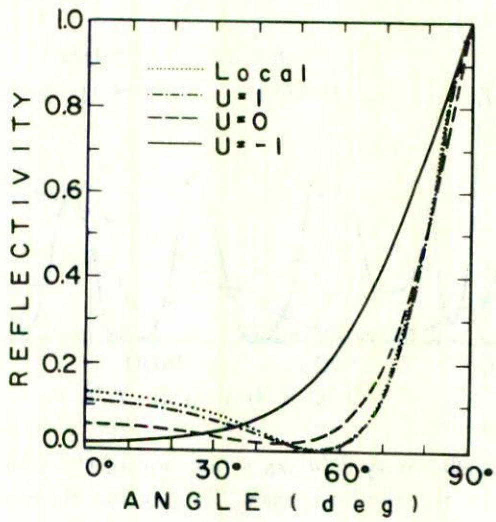

FIGURE 4. Angular scan: the reflectivity $R(\theta)$ as a function of the angle of incidence for three ABC's and the local case. The parameters are the same as in Fig. 2 and $\omega = \omega_L$.

4.4. *Transmission and absorption*

The transmittivity $T(\omega)$, given by Eqs. (30) and (31) has been calculated for the same case that we considered in sec. 4.2. The normal incidence spectrum is shown in Fig. 6. Again, the non-local effects are very weak for $U = 1$ and they are very prominent for $U = -1$. As we proceed from $U = 1$ to $U = -1$ the transmittivity between ω_T and ω_L increases, demonstrating that the overall decrease in $R(\omega)$ in this region is not only a result of an increase in the absorptivity. For oblique incidence, $\theta = 80°$, $T(\omega)$ is given in Fig. 7.

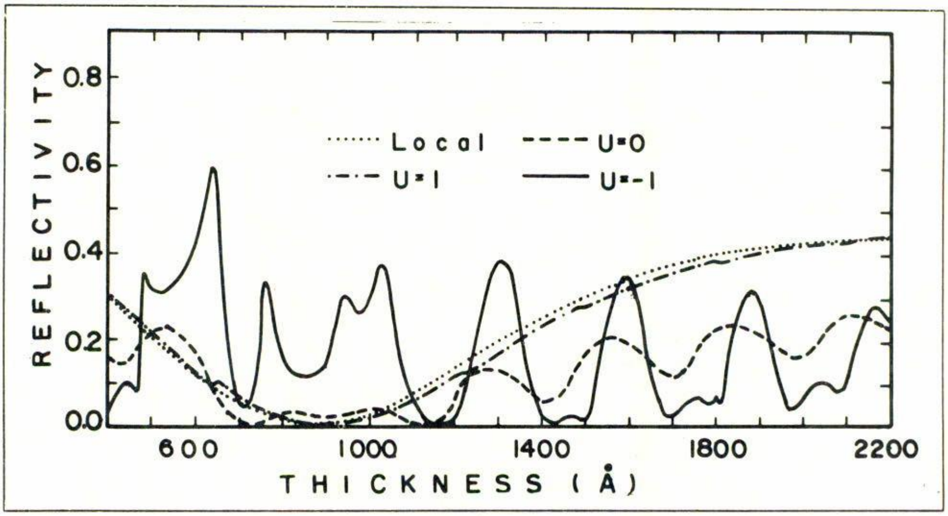

FIGURE 5. The reflectivity $R(d)$ as a function of the film thickness d for three ABC's and the local case. The parameters are the same as in Fig. 2 and $\omega = \omega_L$.

The absorptivity $A(\omega)$ for normal incidence has been calculated from Eq. (32) and is shown in Fig. 8. As for $R(\omega)$, resonances now in the form of peaks, rather than minima appear for $\omega > \omega_L$ as the value of U is decreased from 1 to -1. These peaks are consequence of interference of the four partial plane waves.

The positions of the resonances in $R(\omega)$, $T(\omega)$ and $A(\omega)$ coincide, except for $\omega \sim \omega_L$.

4.5. Comparison with an experimental spectrum

In this subsection we perform a comparison of calculated reflectivity spectra with an experimental spectrum of a 2,000 Å thick CdS film, reported by Makarenko *et al.* [8]. We use the parameters found by Yu and Evangelisti [9] and we also allow for exciton-free layers of thickness $l = 100$ Å. The results for $R(\omega)$ in the local case and for five values of U are shown in Fig. 9; the experimental spectrum

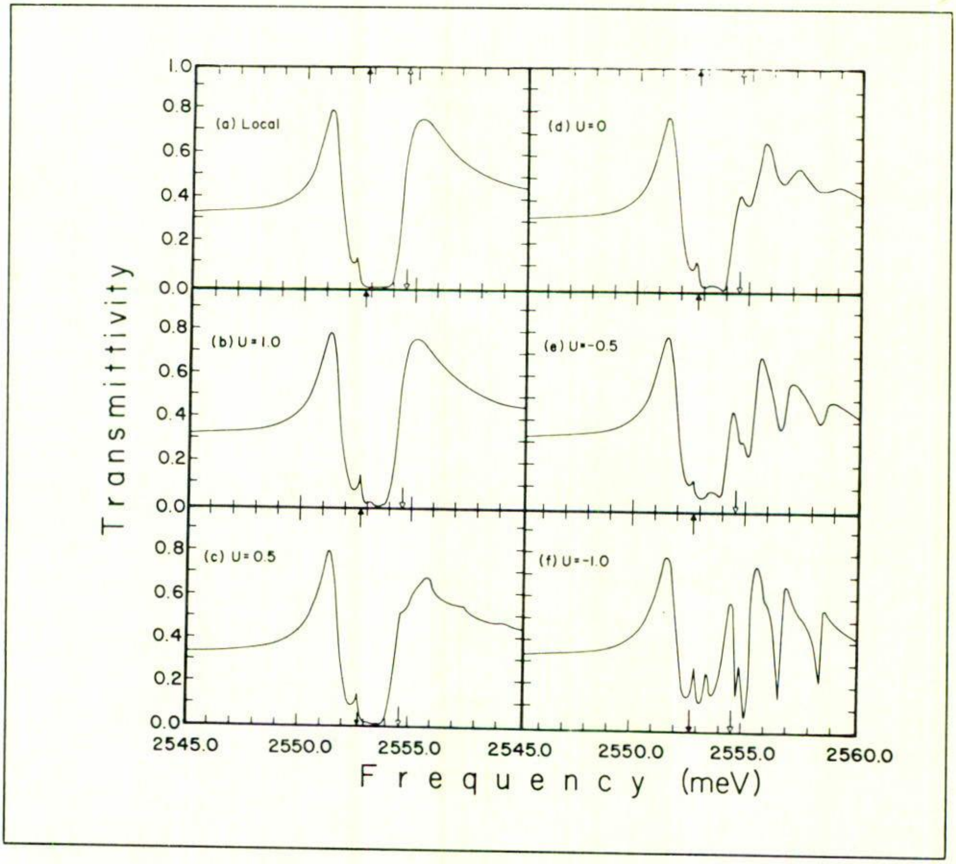

FIGURE 6. Normal incidence transmittivity spectra $T(\omega)$ for the same set of parameters as in Fig. 2.

is also drawn with dashed lines. We observe that for $U = -0.5$ the number of experimentally observed peaks and their relative height are well reproduced. However the theoretical minima are displaced towards lower energies as compared with the experimental minima, and this effect increases for $\omega > \omega_L$. For $U = -1$ (the Pekar ABC) the positions of the theoretical minima are improved in the region $\omega < \omega_L$, however their width becomes very small for $\omega > \omega_L$. The fit in the vicinity of ω_L improves if the thickness of the dead layer is

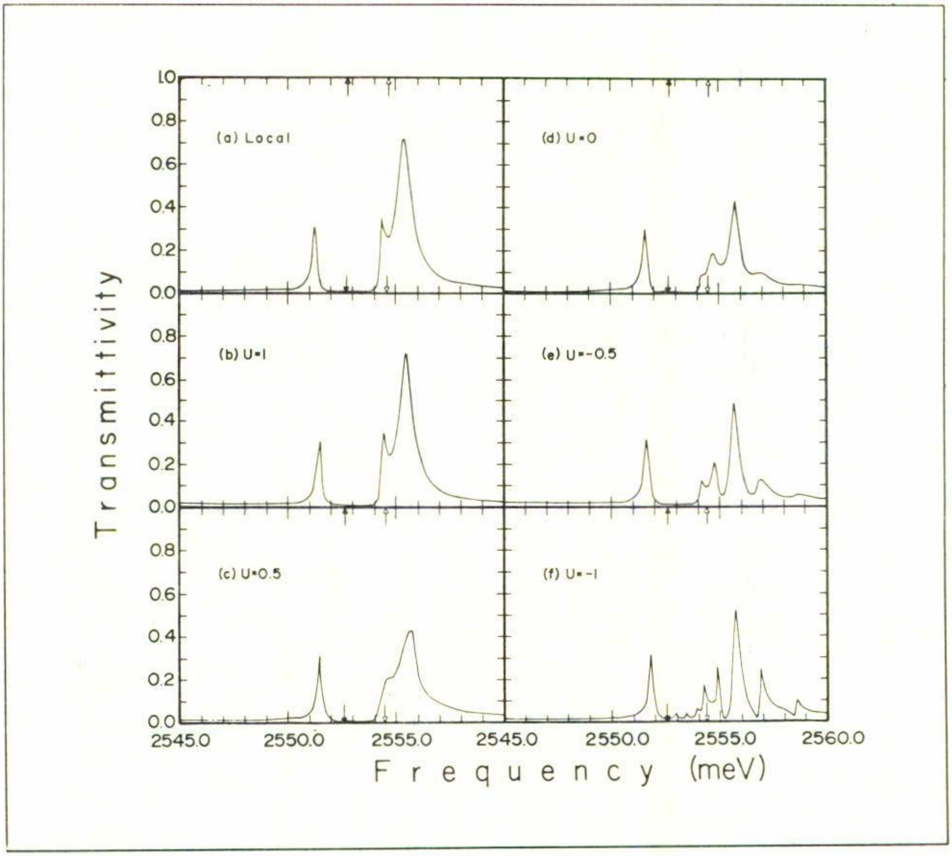

FIGURE 7. As in Fig. 6 for *s*-polarized light with an angle of incidence $\theta = 80°$.

reduced to 80 Å. We note that, for a surface, the Pekar ABC gave a very good agreement with an experimental spectrum.

5. Discussion

The spectra shown in Figs. 2–9 are results of a complicated interference of four plane waves with wavevectors $\pm q_1$ and $\pm q_2$ and amplitudes that depend on the ABC. The strongest effects of spatial

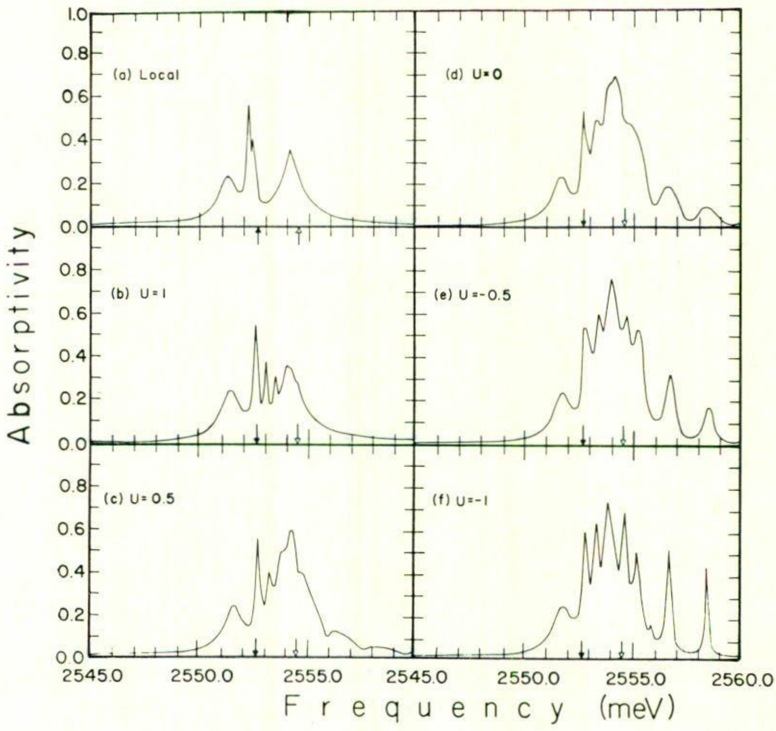

FIGURE 8. Normal-incidence absorptivity spectra $A(\omega)$ for the same set of parameters as in Fig. 2.

dispersion are found for $U = -1$ (the Pekar ABC), and the weakest for $U = 1$ (the Fuchs–Kliewer or Ting *et al.* ABC). The positions of the resonances are strongly affected by the mass of the exciton.

We also find that our inclusion of dead layers at both surfaces of the film strongly affects the spectra. This is to be expected because these layers comprise a sizeable fraction ($2l/d = 1/6$) of the overall width of our film ($d = 1,200$ Å). The allowance for exciton-free layers may substantially alter best-fit values of parameters such as the

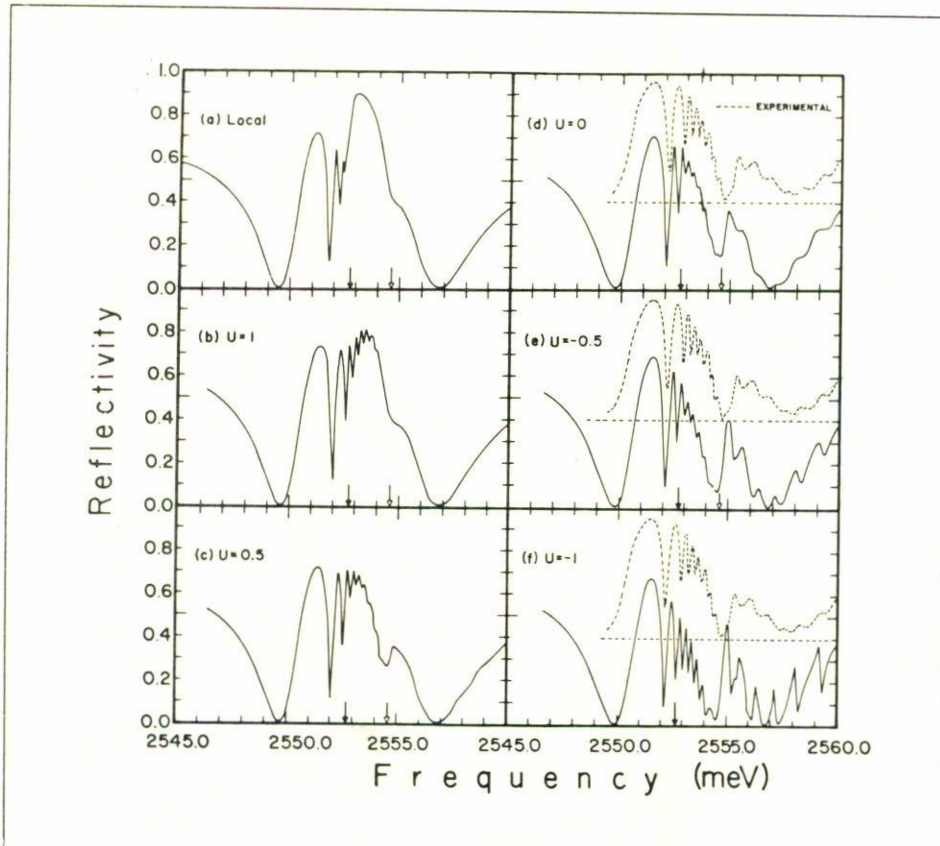

FIGURE 9. Comparison of calculated, normal-incidence reflectivity spectra $R(\omega)$ with an experimental spectrum for the $A(n = 1)$ exciton of CdS (Makarenko *et al.* [8]). The film thickness is 2,000 Å; all the other parameters are the same as in Fig. 2. The ABC corresponding to $U = -0.5$ gives a reasonable fit to the experimental curve.

exciton mass, deduced from experimental spectra. We have studied the dependence of the reflectivity on the dead-layer thickness l for a 2,000 Å thick film. As l is increased from 20 Å to 100 Å considerable changes occur in $R(\omega)$:

(a) There is a major shift, +0.7 meV, of the broad, low-energy minimum.

(b) The other minima and maxima below ω_L do not suffer large shifts (~ 0.2 meV), however, as we approach ω_L the overall decrease of $R(\omega)$ is much more rapid for $l = 100$ Å than for $l = 20$ Å.

(c) The last two minima, just below ω_L, are absent for $l = 100$ Å; it seems that the last three minima for $l = 20$ Å have merged into a single minimum (the last below ω_L).

(d) Just above ω_L the spectra for $l = 20$ Å and $l = 100$ Å are qualitatively different. The first peak (at $\sim 2,555$ meV) is much more prominent in the latter case.

(e) The positions of the minima above ω_L shift to higher frequencies as we increase l from 0 to 100 Å. The shift increases with $(\omega - \omega_T)$ and, for sufficiently high frequencies, is well accounted for by the formula

$$\Delta\omega_n \simeq 4(\omega_n - \omega_T)\Delta l/(d - 2l). \qquad (35)$$

This is obtained from Eq. (34) by calculating the change in a resonance frequency ω_n due to a change Δl in l. We assumed that, well above ω_T, the nonlocal polariton branch may be approximated by the bare exciton dispersion, namely $\omega = \omega_T + \hbar q^2/2m$.

(f) While the individual minima above ω_L shift to higher frequencies, the overall (smoothed-out) structure shifts ~ 1 meV to lower frequencies.

On the basis of a microscopic approach D'Andrea and Del Sole [16] claimed that $l = 18$ Å for CdS, rather than ~ 100 Å as believed by most workers in the field. Our discussion above, along with experimental work on high-quality thin films, should settle this point. However, we should mention that an exciton-free layer is actually an approximation to a continuously varying surface potential. Continuous models of transition layers have been recently applied *to surfaces* by D'Andrea and Del Sole [16], R. Ruppin and R. Englman [17], and Gotthard, Stahl, and Czaijkowski [18].

We have also studied the effect of the damping frequency ν on the spectra. As ν is increased from 0.062 meV, through 0.124 meV, to 0.248 meV the smaller peaks become shoulders and ultimately disappear. The increase of ν by a factor of four results in a very notable smoothing out of the spectrum. However, the positions of the peaks and minima remain practically unchanged. As may be expected, there is an overall decrease, with ν of $R(\omega)$; the peak at 2,555 meV decreases disproportionately, by a factor of two. The changes are most pronounced in the vicinity of ω_L.

Our comparison with an experimental reflectivity spectrum (Makarenko [8]) favors a parameter $U = -0.5$ that corresponds to an ABC which occupies an intermediate position between the Pekar ABC ($U = -1$) and the Agarwal *et al.* ABC ($U = 0$). On the other hand, Makarenko *et al.* preferred the Pekar ABC with a discontinuous jump of the damping frequency ν at $\omega \simeq \omega_L$, which procedure also gives theoretical spectra that compare well with the experimental ones.

Acknowledgements

We wish to thank R. Fuchs and G. Hernandez-Cocoletzi for useful discussions. This research was supported by Consejo Nacional de Ciencia y Tecnología, The Secretaría de Educación Pública, and a cooperative program between the Universidad de Sonora and the Universidad Autónoma de Puebla.

Appendix A. Calculation of the surface impedance Z

We will calculate the surface impedance Z, that appears in the Eq. (22), in terms of a sequence of surface impedances at $z = l^+$, $d - 2l^+$, and d^+.

From Eqs. (21*b*) and (25) one finds for $z = 0$:

$$Z(0^+) = \frac{q_0}{q_l} \frac{1 + E_1^{(-)}/E_1^{(+)}}{1 - E_1^{(-)}/E_1^{(+)}}; \tag{A.1}$$

in the same way for $z = l$

$$Z(l) = \frac{q_0}{q_l}\,\frac{1 + [E_1^{(-)}/E_1^{(+)}]\,e^{-2iq_l l}}{1 - [E_1^{(-)}/E_1^{(+)}]\,e^{-2iq_l l}}. \tag{A.2}$$

From Eqs. (A.1) and (A.2) one obtains $Z(0^+)$ in terms of $Z(l)$, Eq. (26) of the text:

$$Z = Z(0^+) = \frac{q_0}{q_l}\,\frac{Z(l) - i(q_0/q_l)\tan q_l l}{(q_0/q_l) - iZ(l)\tan q_l l}. \tag{26}$$

Substituting Eq. (5a) in Eq. (25) with $z = l$ and then with $z = d - l$ one finds the expressions

$$Z(l) = \frac{\sum_{k=1}^{2}\left[E^{(+k)}e^{iq_k l} + E^{(-k)}e^{-iq_k l}\right]}{\sum_{k=1}^{2}\left\{\frac{q_k}{q_0}\left[E^{(+k)}e^{iq_k l} - E^{(-k)}e^{-iq_k l}\right]\right\}} \tag{A.3}$$

and

$$Z(d-l) = \frac{\sum_{k=1}^{2}\left[E^{(+k)}e^{iq_k(d-l)} + E^{(-k)}e^{-iq_k(d-l)}\right]}{\sum_{k=1}^{2}\left\{\frac{q_k}{q_0}\left[E^{(+k)}e^{iq_k(d-l)} - E^{(-k)}e^{-iq_k(d-l)}\right]\right\}}. \tag{A.4}$$

To relate the last two expressions, one eliminates $E^{(-1)}$ and $E^{(-2)}$ from the ABC's, Eqs. (15) and (16):

$$E^{(-1)} = \xi_1 E^{(+1)} + \xi_2 E^{(+2)}, \tag{A.5}$$

$$E^{(-2)} = n_1 E^{(+1)} + n_2 E^{(+2)}, \tag{A.6}$$

where

$$\xi_1 = \frac{1}{\psi}\Big[a(q_2)a(q_1)e^{i(q_1+q_2)l} - a(-q_2)a(-q_1)e^{i(q_1+q_2)(d-l)}\Big]e^{-i(q_2-q_1)d}, \tag{A.7a}$$

$$\xi_2 = \frac{1}{\psi}\left[a^2(q_2)e^{2iq_2 l} - a^2(-q_2)e^{2iq_2(d-l)}\right]e^{-i(q_2-q_1)d}, \tag{A.7b}$$

$$n_1 = \frac{1}{\psi}\left[a^2(-q_1)e^{2iq_1(d-l)} - a^2(q_1)e^{2iq_1 l}\right], \tag{A.7c}$$

$$n_2 = \frac{1}{\psi}\left[a(-q_2)a(-q_1)e^{i(q_1+q_2)(d-l)} - a(q_2)a(q_1)e^{i(q_1+q_2)l}\right], \tag{A.7d}$$

$$\psi = a(-q_2)a(q_1)e^{-i(q_2-q_1)l} - a(q_2)a(-q_1)e^{-i(q_2-q_1)(d-l)}. \tag{A.7e}$$

Then, substituting $E^{(-1)}$ and $E^{(-2)}$ from Eqs. (A.5) and (A.6) in Eqs. (A.3) and (A.4) one has for $z = l$ and $z = d - l$:

$$Z(l) = \frac{q_0\left[b_1 + b_2\frac{E^{(+2)}}{E^{(+1)}}\right]}{b_3 - b_4\frac{E^{(+2)}}{E^{(+1)}}} \tag{A.8}$$

and

$$Z(d-l) = \frac{q_0\left[c_1 + c_2\frac{E^{(+2)}}{E^{(+1)}}\right]}{c_3 - c_4\frac{E^{(+2)}}{E^{(+1)}}}, \tag{A.9}$$

where

$$\begin{aligned} b_1 &= f(q_1, q_2, \xi_1, n_1, l), & c_1 &= f(q_1, q_2, \xi_1, n_1, d-l),\\ b_2 &= f(q_2, q_1, n_2, \xi_2, l), & c_2 &= f(q_2, q_1, n_2, \xi_2, d-l),\\ b_3 &= g(q_1, q_2, \xi_1, n_1, l), & c_3 &= g(q_1, q_2, \xi_1, n_1, d-l),\\ b_4 &= -g(q_2, q_1, n_2, \xi_2, l), & c_4 &= -g(q_2, q_1, n_2, \xi_2, d-l), \end{aligned} \tag{A.10}$$

and

$$f(x_1, x_2, y_1, y_2, L) = e^{ix_1 L} + y_1 e^{-ix_1 L} + y_2 e^{-ix_2 L}, \tag{A.11a}$$

$$g(x_1, x_2, y_1, y_2, E) = x_1\left(e^{ix_1 L} - y_1 e^{-ix_1 L} - x_2 y_2 e^{-ix_2 L}\right). \tag{A.11b}$$

Then, from Eqs. (A.8) and (A.9), one obtains the Eq. (27) of text:

$$Z(l) = q_0\frac{b_1}{b_3}\,\frac{(b_1+b_2)Z(d-l) + q_0(b_1c_2/c_4 - b_2c_1/c_3)}{(b_3-b_4)Z(d-l) + q_0(b_3c_2/c_4 + b_4c_1/c_3)}, \tag{27}$$

From Eqs. (21c) and (25) one obtains for $z = d - l$ and $z = d$ respectively:

$$Z(d-l) = \frac{q_0}{q_l} \frac{1 + [E_2^{(-)}/E_2^{(+)}]e^{-2iq_l(d-l)}}{1 - [E_2^{(-)}/E_2^{(+)}]e^{-2iq_l(d-l)}}. \qquad (A.12)$$

and

$$Z(d) = \frac{q_0}{q_l} \frac{1 + [E_2^{(-)}/E_2^{(+)}]e^{-2iq_l d}}{1 - [E_2^{(-)}/E_2^{(+)}]e^{-2iq_l d}}. \qquad (A.13)$$

Relating the last two equations, $Z(d-l)$ is found in terms of $Z(d)$:

$$Z(d-l) = \frac{q_0}{q_l} \frac{Z(d) - i(q_0/q_l)\tan q_l l}{(q_0/q_l) - iZ(d)\tan q_l l}. \qquad (28)$$

Finally, from Eqs. (21d) and (25), $Z(d)$ can be written

$$Z(d) = Z^{(0)} = 1/\cos\theta. \qquad (29)$$

Appendix B. Calculation of E_T/E_I

To obtain the ratio E_T/E_I we decompose it in the form

$$\frac{E_T}{E_I} = \frac{E_T}{E_2^{(+)}} \frac{E_2^{(+)}}{E^{(+1)}} \frac{E^{(+1)}}{E_1^{(+)}} \frac{E_1^{(+)}}{E_I}. \qquad (B.1)$$

From the continuity conditions for $E(z)$ at $z = d$ and the Eqs. (21c) and (21d) one obtains

$$\frac{E_T}{E_2^{(+)}} = \left[1 + \frac{E_2^{(-)}}{E_2^{(+)}} e^{-2iq_l d}\right] e^{-iq_0 d\cos\theta} e^{iq_l d}. \qquad (B.2)$$

In a similar way and from Eqs. (A.5)–(A.7) one finds for $z = d - l$

$$\frac{E_2^{(+)}}{E^{(+1)}} = \frac{\left[c_1 + c_2 \frac{E^{(+2)}}{E^{(+1)}}\right] e^{-iq_l(d-l)}}{1 + \left[E_2^{(-)}/E_2^{(+)}\right] e^{-2iq_l(d-l)}}, \tag{B.3}$$

where c_1 and c_2 were defined by Eqs. (A.10).

From the continuity conditions for $E(z)$ at $z = l$ and the Eqs. (21b) and (5a) we have

$$\frac{E^{(+1)}}{E_1^{(+)}} = \frac{\left[1 + \frac{E_1^{(-)}}{E_1^{(+)}} e^{-2iq_l l}\right] e^{iq_l l}}{b_1 + b_2 E^{(+2)}/E^{(+1)}}, \tag{B.4}$$

where b_1 and b_2 were defined by Eqs. (A.10).

In the same way one finds

$$\frac{E_1^{(+)}}{E_I} = \frac{1 + E_R/E_I}{1 + E_1^{(-)}/E_1^{(+)}}. \tag{B.5}$$

Substituting the Eqs. (B.2)–(B.5) in (B.1), the ratio E_T/E_I becomes

$$\frac{E_T}{E_I} = \left(1 + \frac{E_R}{E_I}\right) \frac{1 + \left[E_1^{(-)}/E_1^{(+)}\right] e^{-2iq_l l}}{1 + E_1^{(-)}/E_1^{(+)}} \frac{c_1 + c_2 E^{(+2)}/E^{(+1)}}{b_1 + b_2 E^{(+2)}/E^{(+1)}} \times \frac{1 + \left[E_2^{(-)}/E_2^{(+)}\right] e^{-2iq_l l}}{1 + \left[E_2^{(-)}/E_2^{(+)}\right] e^{-2iq_l(d-l)}} e^{2iq_l l} e^{-iq_0 d \cos\theta}. \tag{B.6}$$

Then, from Eqs. (A.2), (A.13) and (A.9) one obtains, respectively the following expressions:

$$\frac{1 + \left[E_1^{(-)}/E_1^{(+)}\right] e^{-2iq_l l}}{1 + E_1^{(-)}/E_1^{(+)}} = \frac{Z(l) e^{-iq_l l}}{Z(l) \cos q_l l - i(q_0/q_l) \sin q_l l}, \tag{B.7}$$

$$\frac{1+\left[E_2^{(-)}/E_2^{(+)}\right]e^{-2iq_l l}}{1+\left[E_2^{(-)}/E_2^{(+)}\right]e^{-2iq_l(d-l)}}=\frac{Z(d)e^{-iq_l l}}{Z(d)\cos q_l l-i(q_0/q_l)\sin q_l l}, \tag{B.8}$$

and

$$\frac{c_1+c_2E^{(+2)}/E^{(+1)}}{b_1+b_2E^{(+2)}/E^{(+1)}}=\frac{Z(d-l)(c_1c_4+c_2c_3)}{Z(d-l)(b_1c_4+b_2c_3)+q_0(b_1c_2-b_2c_1)}. \tag{B.9}$$

From Eqs. ($21a$) and (24) one finds

$$1+\frac{E_R}{E_I}=\frac{2Z}{Z+Z^{(0)}}. \tag{B.10}$$

Finally, substituting Eqs. (B.7)–(B.10) in the right hand side of Eq. (B.6), one has E_T/E_I in terms of the impedances:

$$\begin{aligned}\frac{E_T}{E_I}=&\left[\frac{2Z}{Z+Z^{(0)}}\right]\left[\frac{Z(l)}{Z(l)\cos q_l l-i(q_0/q_l)\sin q_l l}\right]\\&\times\left[\frac{Z(d-l)(c_1c_4+c_2c_3)}{Z(d-l)(b_1c_4+b_2c_3)+q_0(b_1c_2-b_2c_1)}\right]\\&\left[\frac{Z(d)}{Z(d)\cos q_l l-i(q_0/q_l)\sin q_l l}\right]e^{-iq_0 d\cos\theta}.\end{aligned} \tag{B.11}$$

This is the same as Eq.(31).

References

1. P. Halevi and R. Fuchs, *J. Phys. C: Solid State Physics* **17** (1984) 3869.
2. P. Halevi and R. Fuchs, *J. Phys. C: Solid State Phys.* **17** (1984) 3889.
3. V.A. Kiselev, B.S. Razbirin and I.N. Uraltsev, *Phys. Stat. Sol. (b)* **72** (1975) 161.

4. S.I. Pekar, *Sov. Phys. JETP.* **6** (1958) 785.
5. J.J. Hopfield and D.G.Thomas, *Phys. Rev.* **132** (1963) 563.
6. M.F. Bishop, *Solid State Commun.* **20** (1976) 779.
7. D.L. Johnson, *Phys. Rev. B* **18** (1978) 1942.
8. I.F. Makarenko, I.N. Uraltsev and V.A. Kiselev, *Phys. Stat. Sol. (b)* **98** (1980) 773.
9. P.Y. Yu and F. Evangelisti, *Phys. Rev. Lett.* **42** (1979) 1642.
10. G.S. Agarwal, D.N. Pattanayak and E. Wolf, *Phys. Rev. Lett.* **27** (1971) 1022; *Opt. Commun.* **4** (1971) 255.
11. R. Fuchs and K.L. Kliewer, *Phys. Rev. B* **3** (1971) 2270; K.L. Kliewer and R. Fuchs, *Phys. Rev.* **172** (1968) 607.
12. C.S. Ting, M.J. Frankel and J.L. Birman, *Solid State Commun.* **17** (1975) 1285.
13. M. Born and E. Wolf, *Principles of Optics*, Pergamon 6th corrected ed. (1983).
14. J.A. Gaspar-Armenta (1983) M.Sc. Thesis, Universidad Autónoma de Puebla.
15. P. Halevi and G. Hernández-Cocoletzi, *Phys. Rev. Lett.* **48** (1982) 1500.
16. A. D'Andrea and R. Del Sole, *Phys. Rev. B* **29** (1984) 4782.
17. R. Ruppin and R. Englman, *Phys. Rev. Lett.* **53** (1984) 1688.
18. L. Gotthard, A. Stahl and G. Czaijkowski, *J. Phys. C: Solid State Phys.* **17** (1984) 4865.